Journal of
Mechanics of
Materials and Structures

VARIABLE HORIZON IN A PERIDYNAMIC MEDIUM

Stewart A. Silling, David J. Littlewood and Pablo Seleson

msp

msp

VARIABLE HORIZON IN A PERIDYNAMIC MEDIUM

STEWART A. SILLING, DAVID J. LITTLEWOOD AND PABLO SELESON

A notion of material homogeneity is proposed for peridynamic bodies with variable horizon but constant bulk properties. A relation is derived that scales the force state according to the position-dependent horizon while keeping the bulk properties unchanged. Using this scaling relation, if the horizon depends on position, artifacts called ghost forces may arise in a body under a homogeneous deformation. These artifacts depend on the second derivative of the horizon and can be reduced by employing a modified equilibrium equation using a new quantity called the *partial stress*. Bodies with piecewise constant horizon can be modeled without ghost forces by using a simpler technique called a *splice*. As a limiting case of zero horizon, both the partial stress and splice techniques can be used to achieve local–nonlocal coupling. Computational examples, including dynamic fracture in a one-dimensional model with local–nonlocal coupling, illustrate the methods.

1. Introduction

The peridynamic theory is a strongly nonlocal formulation of solid mechanics, based on long-range forces, that is adapted to the study of continuous bodies with evolving discontinuities, including cracks [Silling 2000; Silling et al. 2007; Silling and Lehoucq 2010]. Each material point x in the reference configuration of a body $\mathcal{B}$ interacts through the material model with other material points within a distance $\delta(x)$ of itself. The maximum interaction distance $\delta(x)$ is called the *horizon* of x. The material points within the horizon of x comprise a set called the *material family* of x:

$$\mathcal{F}_x = \{q \in \mathcal{B} : 0 < |q - x| \le \delta(x)\},$$

where $|\cdot|$ denotes the Euclidean norm. The vector from x to any neighboring material point $q \in \mathcal{F}_x$, $\xi = q - x$, is called a *bond*. The set of bonds from x to its neighbors within its horizon is called the *family* of x, denoted $\mathcal{H}_x$:

$$\mathcal{H}_x = \{\xi \in \mathbb{R}^3 : x + \xi \in \mathcal{F}_x\}.$$

In an elastic peridynamic solid, the strain energy density $W(x)$ is determined by the collective deformation of $\mathcal{F}_x$. To express this collective deformation, it is convenient to define the function

$$\underline{Y}[x, t]\langle \cdot \rangle : \mathcal{H}_x \to \mathbb{R}^3$$

that maps bonds into their images under the deformation y. For any material point $q \in \mathcal{F}_x$ at time $t \ge 0$, let

$$\underline{Y}[x, t]\langle q - x \rangle = y(q, t) - y(x, t). \tag{1-1}$$

The function $\underline{Y}[x, t]\langle \cdot \rangle$ is an example of a *state*, which is a mapping with domain $\mathcal{H}_x$. By convention, the bond $\xi \in \mathcal{H}_x$ that a state operates on is written in angle brackets, i.e., $\langle \xi \rangle$. The state $\underline{Y}[x, t]$ is called the *deformation state* at x and at time t. The deformation state is the basic kinematical quantity for purposes of material modeling, and, in this role, it is analogous to the deformation gradient in the classical theory of continuum mechanics, $F = \partial y / \partial x$.

In the present discussion, for convenience, we will adopt the generalization that a state operating on a bond vector outside of the family of a given point x is defined, but its value is zero:

$$|\xi| > \delta(x) \Longrightarrow \underline{A}[x]\langle \xi \rangle = \mathbf{0}.$$

The inner product of two states $\underline{A}$ and $\underline{B}$ is defined by

$$\underline{A} \bullet \underline{B} = \int_{\mathcal{H}} \underline{A}\langle \xi \rangle \cdot \underline{B}\langle \xi \rangle \, dV_{\xi}. \tag{1-2}$$

In (1-2) and the rest of this paper, we use the symbol $\mathcal{H}$ instead of $\mathcal{H}_x$ when it is not necessary to refer to a specific $x \in \mathcal{B}$. The *norm* of a state $\underline{A}$ is defined by

$$\|\underline{A}\| = \sqrt{\underline{A} \bullet \underline{A}}.$$

In an elastic material, the strain energy density $W(x)$ depends through the material model on the deformation state, and this dependence is written as

$$W(x) = \widehat{W}(\underline{Y}[x]).$$

When manipulating functions of states such as W, it is helpful to introduce the *Fréchet derivative*. Given the function $\widehat{W}(\underline{Y})$, its Fréchet derivative $\widehat{W}_{\underline{Y}}$ is a functional derivative with the property that if $\delta \underline{Y}$ is a small increment in the deformation state, then

$$\widehat{W}(\underline{Y} + \delta \underline{Y}) = \widehat{W}(\underline{Y}) + \widehat{W}_{\underline{Y}}(\underline{Y}) \bullet \delta \underline{Y} + o(\|\delta \underline{Y}\|). \tag{1-3}$$

Note that $\widehat{W}_{\underline{Y}}$ is a state-valued function even though $\widehat{W}$ is scalar-valued.

Let Φ_y denote the total potential energy in a bounded elastic body $\mathcal{B}$ under external force density field b, subjected to the deformation y:

$$\Phi_y = \int_{\mathcal{B}} (W(x) - b(x) \cdot y(x)) \, dV_x. \tag{1-4}$$

To derive the Euler–Lagrange equation corresponding to stationary values of this functional, set the first variation of (1-4) to zero. Combining (1-1), (1-3), and (1-4), and neglecting higher-order terms in the small increment in the deformation state, leads to

$$\begin{aligned}
0 = \delta \Phi_y &= \int_{\mathcal{B}} (\delta W(x) - b(x) \cdot \delta y(x)) \, dV_x \\
&= \int_{\mathcal{B}} (\widehat{W}_{\underline{Y}}(\underline{Y}[x]) \bullet \delta \underline{Y}[x] - b(x) \cdot \delta y(x)) \, dV_x \\
&= \int_{\mathcal{B}} \left(\int_{\mathcal{B}} \widehat{W}_{\underline{Y}}(\underline{Y}[x])\langle q - x \rangle \cdot (\delta y(q) - \delta y(x)) \, dV_q - b(x) \cdot \delta y(x) \right) dV_x.
\end{aligned}$$

Using the change of dummy variables $q \leftrightarrow x$ to eliminate $\delta y(q)$, we obtain

$$0 = \int_{\mathcal{B}} \left(\int_{\mathcal{B}} (\widehat{W}_{\underline{Y}}(\underline{Y}[q]) \langle x - q \rangle - \widehat{W}_{\underline{Y}}(\underline{Y}[x]) \langle q - x \rangle) \, dV_q - b(x) \right) \cdot \delta y(x) \, dV_x.$$

Since this must hold for every choice of the variation δy, the Euler–Lagrange equation, which is the peridynamic equilibrium equation, is given by

$$L^{\mathrm{pd}}(x) + b(x) = 0 \tag{1-5}$$

for all $x \in \mathcal{B}$. In (1-5), the *peridynamic internal force density* at x is given by

$$L^{\mathrm{pd}}(x) := \int_{\mathcal{B}} \{\underline{T}[x]\langle q - x \rangle - \underline{T}[q]\langle x - q \rangle\} \, dV_q, \tag{1-6}$$

where $\underline{T}[x]$ is the *force state* at x, which is related to the strain energy density by

$$\underline{T}[x] = \widehat{W}_{\underline{Y}}(\underline{Y}[x]). \tag{1-7}$$

The *pairwise bond force density* f on a point x due to its interaction with any point $q \in \mathcal{F}_x$ is given by

$$f(q, x) = \underline{T}[x]\langle q - x \rangle - \underline{T}[q]\langle x - q \rangle. \tag{1-8}$$

The peridynamic internal force density (1-6) may be written more succinctly in terms of the pairwise bond force density as

$$L^{\mathrm{pd}}(x) = \int_{\mathcal{B}} f(q, x) \, dV_q. \tag{1-9}$$

In general,

$$\underline{T}[x] = \widehat{\underline{T}}(\underline{Y}[x]) \quad \text{and} \quad \underline{T}[q] = \widehat{\underline{T}}(\underline{Y}[q]),$$

where $\widehat{\underline{T}}$ is the material model expressed in terms of the force state.

By invoking d'Alembert's principle, the dynamic form of the balance of linear momentum is found from (1-5) to be

$$\rho(x)\ddot{y}(x, t) = L^{\mathrm{pd}}(x, t) + b(x, t) \tag{1-10}$$

for all $x \in \mathcal{B}$ and for any $t \geq 0$, where ρ is the mass density.

The mechanical interpretation of the force state is that $\underline{T}[x]\langle q - x \rangle$ represents a bond force density on x due to its interaction with q. More general material models, whether elastic or not, may be written in the form

$$\underline{T}[x] = \widehat{\underline{T}}(\underline{Y}[x], \ldots, x),$$

where $\widehat{\underline{T}}$ is the material model, which may depend on additional variables besides $\underline{Y}$. The dimensions of $\underline{T}$ and f are force per unit volume squared. The dimensions of W are the same as in the classical theory, i.e., energy per unit volume.

If at any x, $\underline{T}$ depends only on $\underline{Y}$ and x (but not additional variables such as loading history), then the material model is *simple*, and we write

$$\underline{T}[x] = \widehat{\underline{T}}(\underline{Y}[x], x).$$

All elastic materials are simple.

If $\widehat{\underline{T}}$ has no explicit dependence on $\boldsymbol{x}$, then the body is *homogeneous*. If it is simple and homogeneous, we write

$$\underline{T}[\boldsymbol{x}] = \widehat{\underline{T}}(\underline{Y}[\boldsymbol{x}]).$$

Since δ is in effect a material property, any homogeneous body has constant δ.

If δ is constant in $\mathcal{B}$, then the region of integration in (1-6) and (1-9) may be changed from $\mathcal{B}$ to $\mathcal{F}_{\boldsymbol{x}}$. The vast majority of applications of peridynamics to date assume constant horizon.

2. The peridynamic stress tensor

As shown in [Lehoucq and Silling 2008], given a continuously differentiable pairwise bond force density $\boldsymbol{f}$ with asymptotic second-order decay with the bond length, the peridynamic internal force density can be expressed as

$$\boldsymbol{L}^{\mathrm{pd}} = \nabla \cdot \nu^{\mathrm{pd}} \quad \text{in } \mathcal{B},$$

where ν^{pd} is the *peridynamic stress tensor* field defined for any $\boldsymbol{x}$ by

$$\nu^{\mathrm{pd}}(\boldsymbol{x}) := \frac{1}{2} \int_{\mathcal{S}} \int_0^\infty \int_0^\infty (v+w)^2 \boldsymbol{f}(\boldsymbol{x}+v\boldsymbol{m}, \boldsymbol{x}-w\boldsymbol{m}) \otimes \boldsymbol{m} \, dw \, dv \, d\Omega_{\boldsymbol{m}}, \tag{2-1}$$

where $\mathcal{S}$ is the unit sphere, $d\Omega_{\boldsymbol{m}}$ is a differential solid angle in the direction of the unit vector $\boldsymbol{m}$, and $\boldsymbol{f}$ is given by (1-8).

Suppose the deformation is continuously differentiable, and let $\boldsymbol{F}$ be the classical deformation gradient tensor field,

$$\boldsymbol{F} = \nabla \boldsymbol{y} \quad \text{in } \mathcal{B}.$$

Define the *deformation gradient state* field $\underline{\boldsymbol{F}}$ by

$$\underline{\boldsymbol{F}}[\boldsymbol{x}]\langle \boldsymbol{\xi} \rangle = \boldsymbol{F}(\boldsymbol{x})\boldsymbol{\xi} \quad \text{for all } \boldsymbol{x} \in \mathcal{B} \text{ and } \boldsymbol{\xi} \in \mathcal{H}_{\boldsymbol{x}}. \tag{2-2}$$

An equivalent statement to (2-2) is

$$\underline{\boldsymbol{F}} = \boldsymbol{F}\underline{\boldsymbol{X}} \quad \text{in } \mathcal{B},$$

where $\underline{\boldsymbol{X}}$ is the *identity* state defined by

$$\underline{\boldsymbol{X}}\langle \boldsymbol{\xi} \rangle = \boldsymbol{\xi} \quad \text{for all } \boldsymbol{\xi} \in \mathcal{H}_{\boldsymbol{x}}.$$

Suppose the deformation is such that there is a tensor $\boldsymbol{F}^*$ such that

$$\boldsymbol{y}(\boldsymbol{x}+\boldsymbol{\xi}) - \boldsymbol{y}(\boldsymbol{x}) = \boldsymbol{F}^*\boldsymbol{\xi} \quad \text{for all } \boldsymbol{x} \in \mathcal{B} \text{ and } \boldsymbol{\xi} \in \mathcal{H}_{\boldsymbol{x}}.$$

Then the deformation is called *uniform*. In this case,

$$\underline{\boldsymbol{Y}} = \underline{\boldsymbol{F}} \quad \text{in } \mathcal{B} \quad \text{and} \quad \underline{\boldsymbol{F}}[\boldsymbol{x}]\langle \boldsymbol{\xi} \rangle = \boldsymbol{F}^*\boldsymbol{\xi} \quad \text{for all } \boldsymbol{x} \in \mathcal{B} \text{ and } \boldsymbol{\xi} \in \mathcal{H}_{\boldsymbol{x}}. \tag{2-3}$$

If the body is homogeneous and the deformation is uniform, then the peridynamic stress tensor is easily computed making use of the change of variables $z = v + w$:

$$
\begin{aligned}
\nu^{\mathrm{pd}} &= \int_{\mathcal{S}} \int_0^\infty \int_v^\infty z^2 \widehat{\underline{T}}(\underline{F})\langle z\boldsymbol{m}\rangle \otimes \boldsymbol{m}\, dz\, dv\, d\Omega_{\boldsymbol{m}} \\
&= \int_{\mathcal{S}} \int_0^\infty \int_0^z z^2 \widehat{\underline{T}}(\underline{F})\langle z\boldsymbol{m}\rangle \otimes \boldsymbol{m}\, dv\, dz\, d\Omega_{\boldsymbol{m}} \\
&= \int_{\mathcal{S}} \int_0^\infty z^3 \widehat{\underline{T}}(\underline{F})\langle z\boldsymbol{m}\rangle \otimes \boldsymbol{m}\, dz\, d\Omega_{\boldsymbol{m}} \\
&= \int_{\mathcal{S}} \int_0^\infty \widehat{\underline{T}}(\underline{F})\langle z\boldsymbol{m}\rangle \otimes (z\boldsymbol{m})(z^2\, dz\, d\Omega_{\boldsymbol{m}}) \\
&= \nu^0,
\end{aligned}
\tag{2-4}
$$

where ν^0 is the *collapsed stress tensor* defined by

$$
\nu^0 := \int_{\mathcal{H}} \widehat{\underline{T}}(\underline{F})\langle \boldsymbol{\xi}\rangle \otimes \boldsymbol{\xi}\, dV_{\boldsymbol{\xi}}. \tag{2-5}
$$

Also define the *collapsed internal force density* field by

$$
\boldsymbol{L}^0 := \nabla \cdot \nu^0 \quad \text{in } \mathcal{B}. \tag{2-6}
$$

As discussed in [Silling and Lehoucq 2008], the collapsed stress tensor is an admissible first Piola–Kirchhoff stress tensor whose constitutive model depends on the local deformation gradient tensor through (2-5). The collapsed internal force density field provides the "local limit of peridynamics" in the sense that as $\delta \to 0$,

$$
\boldsymbol{L}^{\mathrm{pd}} \to \boldsymbol{L}^0,
$$

provided that the deformation is twice continuously differentiable and $\widehat{\underline{T}}$ obeys the scaling relation derived in the next section.

3. Rescaling a material model at a point

The remainder of this paper concerns methods for allowing changes in the horizon as a function of position such that the "bulk properties" are invariant to this change. The first step is to specify what this required invariance means.

Suppose an elastic material model is given for a particular value of horizon (without loss of generality, we will assume that this horizon has the value 1), and denote the corresponding strain energy density function by $\hat{W}_1$. Now consider a different value of horizon, δ, and denote the corresponding strain energy density function by $\hat{W}$. As a physical requirement, the strain energy density for any uniform deformation must be invariant with respect to changes in δ. By reasoning similar to that in [Silling and Lehoucq 2008], it is assumed that for any deformation state $\underline{Y}$,

$$
\widehat{W}(\underline{Y}) = \widehat{W}_1(\underline{Y}_1), \tag{3-1}
$$

where $\underline{Y}_1$ is the *reference deformation state* defined by

$$\underline{Y}_1\langle\boldsymbol{n}\rangle := \delta^{-1}\underline{Y}\langle\delta\boldsymbol{n}\rangle \quad \text{for all } \boldsymbol{n} \in \mathcal{H}_1, \tag{3-2}$$

where $\mathcal{H}_1$ is the family of $\boldsymbol{x}$ with horizon 1. In the remainder of this paper, the symbols $\boldsymbol{n}$ or $\boldsymbol{m}$ will generally be used instead of $\boldsymbol{\xi}$ to denote bonds in $\mathcal{H}_1$. To derive the force state $\underline{T}$, observe that (3-1) implies

$$\hat{W}_{\underline{Y}} \bullet d\underline{Y} = (\hat{W}_1)_{\underline{Y}_1} \bullet d\underline{Y}_1.$$

Hence, using (1-7),

$$\underline{T} \bullet d\underline{Y} = \underline{T}_1 \bullet d\underline{Y}_1.$$

Combining this with (1-2), (1-3), and (3-2) leads to the following scaling relation for peridynamic material models in three dimensions:

$$\underline{\hat{T}}(\underline{Y})\langle\boldsymbol{\xi}\rangle = \delta^{-4}\underline{\hat{T}}_1(\underline{Y}_1)\langle\delta^{-1}\boldsymbol{\xi}\rangle \quad \text{for all } \boldsymbol{\xi} \in \mathcal{H}$$

for any deformation state $\underline{Y}$ on $\mathcal{H}$. Repeating the above derivation for one- or two-dimensional models leads to

$$\underline{\hat{T}}(\underline{Y})\langle\boldsymbol{\xi}\rangle = \delta^{-(1+D)}\underline{\hat{T}}_1(\underline{Y}_1)\langle\delta^{-1}\boldsymbol{\xi}\rangle \quad \text{for all } \boldsymbol{\xi} \in \mathcal{H}, \tag{3-3}$$

where D is the number of dimensions and $\underline{Y}_1$ is given by (3-2). The state $\underline{\hat{T}}_1$ is called the *reference material model*.

From (2-2) and (3-2), the deformation gradient state has the following invariance with respect to changes in δ:

$$\underline{F}_1\langle\boldsymbol{n}\rangle = \delta^{-1}\underline{F}\langle\delta\boldsymbol{n}\rangle = \delta^{-1}\boldsymbol{F}\delta\boldsymbol{n} = \boldsymbol{F}\boldsymbol{n} = \underline{F}\langle\boldsymbol{n}\rangle \quad \text{for all } \boldsymbol{n} \in \mathcal{H}_1.$$

Hence,

$$\underline{F}_1 = \underline{F} \quad \text{in } \mathcal{H} \cap \mathcal{H}_1, \tag{3-4}$$

which is a result that could be anticipated owing to the fact that $\boldsymbol{F}$ is dimensionless. From (2-5), (3-2) and (3-3),

$$\begin{aligned}
v^0 &= \int_{\mathcal{H}} \underline{\hat{T}}(\underline{F})\langle\boldsymbol{\xi}\rangle \otimes \boldsymbol{\xi} \, dV_{\boldsymbol{\xi}} \\
&= \int_{\mathcal{H}_1} \delta^{-(1+D)}\underline{\hat{T}}_1(\underline{F}_1)\langle\boldsymbol{n}\rangle \otimes (\delta\boldsymbol{n})(\delta^D dV_{\boldsymbol{n}}) \\
&= \int_{\mathcal{H}_1} \underline{\hat{T}}_1(\underline{F}_1)\langle\boldsymbol{n}\rangle \otimes \boldsymbol{n} \, dV_{\boldsymbol{n}},
\end{aligned} \tag{3-5}$$

which shows that the collapsed stress tensor is also invariant with respect to changes in δ. Note that this invariance does not require the body to be homogeneous.

4. Variable scale homogeneous bodies

Recall from Section 1 that any homogeneous body necessarily has constant horizon. Therefore, it is necessary to define a relaxed concept of homogeneity that captures the meaning of having a peridynamic body with constant "bulk properties" without adhering to the strict definition of homogeneity. The reference material model defined in Section 3 provides a way to do this.

Definition. Suppose a reference material model $\widehat{\underline{T}}_1$ is given in $\mathcal{B}$, independent of position. In addition, let the horizon $\delta(x)$ be prescribed as a function of position. If, at any $x \in \mathcal{B}$,

$$\widehat{\underline{T}}(\underline{Y}[x], x)\langle \xi \rangle = \frac{1}{(\delta(x))^{1+D}} \, \widehat{\underline{T}}_1(\underline{Y}_1[x])\left\langle \frac{\xi}{\delta(x)} \right\rangle \quad \text{for all } \xi \in \mathcal{H}_x, \tag{4-1}$$

then $\mathcal{B}$ is a *variable scale homogeneous* (VSH) body. Note that a homogeneous body is a VSH body with constant horizon.

By the results of Section 3, an elastic VSH body under uniform deformation has constant W. However, it does *not* necessarily have constant ν^{pd} and is therefore not necessarily in equilibrium in the absence of body forces. (Recall that (2-4) applies only to homogeneous bodies, and homogeneity implies that δ is constant.) As shown in the next section, nonconstant δ in a VSH body leads to *ghost forces* at points where the horizon changes.

5. Ghost forces

We demonstrate that in the absence of body forces, a uniform deformation of a VSH body is not necessarily in equilibrium. To see this, assume a uniform deformation, take δ to be twice continuously differentiable, and compute the net internal force density $L^{\text{pd}}(x)$. Extending the integration domain in (1-6) to the entire space for convenience, and using (4-1), we obtain, for any x,

$$L^{\text{pd}}(x) = \int_{\mathbb{R}^3} \{\underline{T}[x]\langle q - x \rangle - \underline{T}[q]\langle x - q \rangle\} \, dV_q$$

$$= \int_{\mathbb{R}^3} \left\{ \delta^{-(1+D)}(x)\underline{T}_1\langle m \rangle - \delta^{-(1+D)}(q)\underline{T}_1\langle n \rangle \right\} dV_q, \tag{5-1}$$

where

$$m = \frac{q - x}{\delta(x)} \quad \text{and} \quad n = \frac{x - q}{\delta(q)}. \tag{5-2}$$

Holding x fixed,

$$dV_q = \left| \det\left(\frac{\partial m}{\partial q} \right) \right|^{-1} dV_m = \delta^D(x) dV_m, \tag{5-3}$$

$$dV_q = \left| \det\left(\frac{\partial n}{\partial q} \right) \right|^{-1} dV_n = \frac{\delta^D(q)}{1 + n \cdot \nabla\delta(q) + O(|\nabla\delta|^2)} dV_n. \tag{5-4}$$

From (5-1)–(5-4), it follows that

$$L^{\text{pd}}(x) = \int_{\mathbb{R}^3} \frac{\underline{T}_1\langle m \rangle}{\delta(x)} \, dV_m - \int_{\mathbb{R}^3} \frac{\underline{T}_1\langle n \rangle}{\delta(q)} \left(\frac{1}{1 + n \cdot \nabla\delta(q) + O(|\nabla\delta|^2)} \right) dV_n$$

$$= \int_{\mathbb{R}^3} \epsilon(x, q)\underline{T}_1\langle m \rangle \, dV_m, \tag{5-5}$$

where

$$\epsilon(\boldsymbol{x}, \boldsymbol{q}) = \frac{1}{\delta(\boldsymbol{x})} - \frac{1}{\delta(\boldsymbol{q})}\left(\frac{1}{1 + \boldsymbol{n} \cdot \nabla\delta(\boldsymbol{q}) + O(|\nabla\delta|^2)}\right)$$
$$= \frac{1}{\delta(\boldsymbol{x})} - \frac{1}{\delta(\boldsymbol{q}) + \nabla\delta(\boldsymbol{q}) \cdot (\boldsymbol{x} - \boldsymbol{q}) + O(\delta|\nabla\delta|^2)}. \tag{5-6}$$

Now approximate $\delta(\boldsymbol{x})$ by the first three terms of a Taylor expansion around $\boldsymbol{q}$, that is,

$$\delta(\boldsymbol{x}) = \delta(\boldsymbol{q}) + \nabla\delta(\boldsymbol{q}) \cdot (\boldsymbol{x} - \boldsymbol{q}) + \tfrac{1}{2}\nabla\nabla\delta(\boldsymbol{q})(\boldsymbol{\xi} \otimes \boldsymbol{\xi}) + \cdots,$$

where $\boldsymbol{\xi} = \boldsymbol{q} - \boldsymbol{x}$. Using this to eliminate the term $\nabla\delta(\boldsymbol{q}) \cdot (\boldsymbol{x} - \boldsymbol{q})$ in (5-6) leads, after further straightforward manipulations, to

$$\epsilon(\boldsymbol{x}, \boldsymbol{q}) = \frac{1}{\delta(\boldsymbol{x})} - \frac{1}{\delta(\boldsymbol{x}) - \tfrac{1}{2}\nabla\nabla\delta(\boldsymbol{q})(\boldsymbol{\xi} \otimes \boldsymbol{\xi}) + \cdots} = -\tfrac{1}{2}\nabla\nabla\delta(\boldsymbol{q})\boldsymbol{m} \otimes \boldsymbol{m} + \cdots,$$

where $\boldsymbol{m}$ is given by (5-2). From this result and (5-5), the peridynamic internal force density at $\boldsymbol{x}$ is estimated from

$$\boldsymbol{L}^{\text{pd}}(\boldsymbol{x}) = -\frac{1}{2} \int_{\mathbb{R}^3} \nabla\nabla\delta(\boldsymbol{q})(\boldsymbol{m} \otimes \boldsymbol{m})\underline{\boldsymbol{T}}_1\langle\boldsymbol{m}\rangle \, dV_{\boldsymbol{m}} + \cdots.$$

We thus obtain

$$|\boldsymbol{L}^{\text{pd}}(\boldsymbol{x})| \le \frac{1}{2} \int_{\mathbb{R}^3} \max_{\mathcal{H}_{\boldsymbol{x}}} \{|\nabla\nabla\delta|\}|\boldsymbol{m} \otimes \boldsymbol{m}||\underline{\boldsymbol{T}}_1\langle\boldsymbol{m}\rangle| \, dV_{\boldsymbol{m}} + \cdots.$$

Since, by assumption, δ is twice continuously differentiable, and since $|\boldsymbol{m}| \le 1$, this result implies

$$\boldsymbol{L}^{\text{pd}}(\boldsymbol{x}) = O(|\nabla\nabla\delta|)O(\|\underline{\boldsymbol{T}}_1\|). \tag{5-7}$$

The departure from equilibrium represented by nonzero values of $\boldsymbol{L}^{\text{pd}}$ is called *ghost force* and is an artifact of the position dependence of the horizon. Observe that the leading term in the ghost force depends on the *second* derivative of δ. In fact, it can be shown directly that if δ is a linear function of position, then the ghost force vanishes.

An illustration of the effect of ghost force in a VSH bar in equilibrium is shown in Figure 1. The
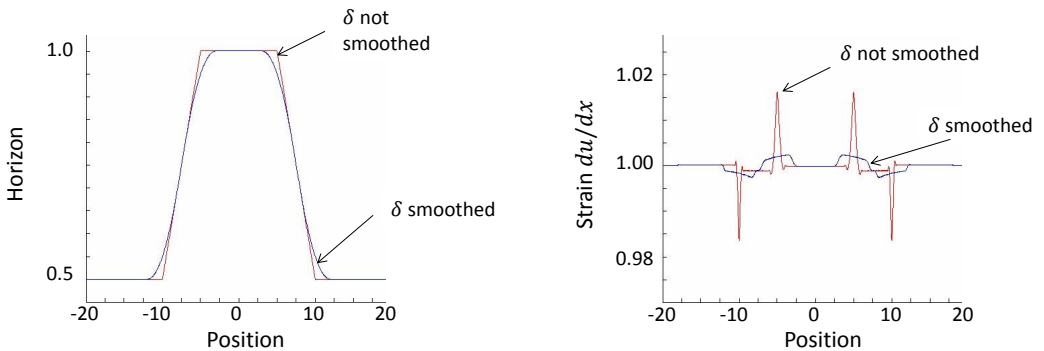
Figure 1. Ghost strain in a VSH body in equilibrium. Left: horizon as a function of position. Right: strain as a function of position.

peridynamic reference material model $\widehat{\underline{T}}_1$ is a bond-based model [Silling 2000] with a nominal Young's modulus of 1. The horizon in the bar depends on position as shown in the left figure. The numerical approximation method is discussed in the Appendix. Two cases are considered for the spatial dependence of the horizon: piecewise linear ("not smoothed") and cubic spline ("smoothed"). The ends of the bar have prescribed displacements corresponding to a nominal strain in the bar of 1. The strain (defined as du/dx) in equilibrium for the two cases is shown in the right figure. The strain is computed numerically using a central finite difference formula. If there were no ghost forces, the strain would be constant and equal to 1. Because of ghost forces, anomalies in strain ("ghost strains") appear that equilibrate the ghost forces. The smoothed $\delta(x)$ has lower ghost strains than the nonsmoothed one. This result is consistent with (5-7), which predicts that ghost forces are proportional to the second derivative of $\delta(x)$.

In this example, the anomalies in strain are less than 2%, even for the nonsmoothed case. This departure from constant strain could be acceptable in many applications. Ghost forces in a VSH peridynamic body are always self-equilibrated, that is, they do not exert a net force on the body. This follows from the fact that the peridynamic equilibrium equation always conserves linear momentum, even if the material model depends on position. To address applications in which these ghost forces are not acceptable, or it is desired to have a jump in $\delta(x)$, we will introduce two methods, *partial stress* and *splice*, that exhibit zero ghost forces in a uniform deformation of a VSH body.

6. The partial stress field

We investigate a modified form of the momentum balance that eliminates ghost forces in a VSH body under a uniform deformation. The momentum balance is expressed in terms of a new field called the "partial stress" tensor field.

Consider a peridynamic body $\mathcal{B}$ and let its force state field $\underline{T}$ be given. Let the *partial stress* tensor field ν^{ps} be defined by

$$\nu^{\mathrm{ps}}(\boldsymbol{x}) := \int_{\mathcal{H}_x} \underline{T}[\boldsymbol{x}]\langle \boldsymbol{\xi} \rangle \otimes \boldsymbol{\xi} \, dV_{\boldsymbol{\xi}} \quad \text{for all } \boldsymbol{x} \in \mathcal{B}. \tag{6-1}$$

Also define the *partial internal force density* by

$$\boldsymbol{L}^{\mathrm{ps}}(\boldsymbol{x}) := \nabla \cdot \nu^{\mathrm{ps}}(\boldsymbol{x}) \quad \text{for all } \boldsymbol{x} \in \mathcal{B}. \tag{6-2}$$

If the material model is simple, the partial stress can be expressed in the form

$$\nu^{\mathrm{ps}}(\boldsymbol{x}) = \widehat{\nu^{\mathrm{ps}}}(\underline{Y}[\boldsymbol{x}]) \quad \text{for all } \boldsymbol{x} \in \mathcal{B},$$

where

$$\widehat{\nu^{\mathrm{ps}}}(\underline{Y}) = \int_{\mathcal{H}} \widehat{\underline{T}}(\underline{Y})\langle \boldsymbol{\xi} \rangle \otimes \boldsymbol{\xi} \, dV_{\boldsymbol{\xi}}. \tag{6-3}$$

Note the similarity between ν^{ps} and ν^0 defined by (2-5). The difference is that ν^{ps} depends on the (nonlocal) deformation state $\underline{Y}$, while ν^0 depends on the (local) deformation gradient tensor. In the special case of a uniform deformation of a homogeneous body (which implies $\delta = \text{constant}$ and $\underline{Y} = \underline{F}$), clearly $\nu^{\mathrm{ps}} \equiv \nu^0$.

By repeating the manipulations leading to (3-5), it is easily shown that in a VSH body with reference material model $\widehat{\underline{T}}_1$,

$$v^{\mathrm{ps}}(\boldsymbol{x}) = \int_{\mathcal{H}_1} \widehat{\underline{T}}_1(\underline{Y}_1[\boldsymbol{x}])\langle \boldsymbol{n}\rangle \otimes \boldsymbol{n}\, dV_{\boldsymbol{n}} \quad \text{for all } \boldsymbol{x} \in \mathcal{B}, \tag{6-4}$$

where $\underline{Y}_1$ is given by (3-2). Since, in a uniform deformation, $\underline{Y}_1$ is constant (and equal to $\underline{F}$), it follows from (2-3), (2-6), (3-4), (3-5), (6-2), and (6-4) that in a VSH body under a uniform deformation,

$$v^{\mathrm{ps}} \equiv v^0 \quad \text{and} \quad \boldsymbol{L}^{\mathrm{ps}} \equiv \boldsymbol{L}^0 \equiv \boldsymbol{0}. \tag{6-5}$$

This establishes that, for a VSH body under a uniform deformation, ghost forces are absent in the partial stress formulation of the momentum balance equation, regardless of the spatial dependence of horizon. This observation motivates the use of this modified momentum balance in the transition region of the horizon.

7. The partial stress as an approximation to peridynamics

With the intent of modeling some parts of a body using the partial internal force density (6-2) and other parts using the peridynamic internal force density (1-6), the relation between the two will now be investigated. Since the plan is to make a transition between $\boldsymbol{L}^{\mathrm{ps}}$ and $\boldsymbol{L}^{\mathrm{pd}}$ where the horizon is constant, we investigate the way these fields approximate each other under this assumption.

Proposition 1. *Let $\mathcal{B}$ be a homogeneous body* (*which implies constant δ*). *Let a twice continuously differentiable deformation $\boldsymbol{y}$ of $\mathcal{B}$ be prescribed. Then*

$$v^{\mathrm{pd}} - v^{\mathrm{ps}} = O(\delta)O(\|\nabla \underline{T}_1\|) \quad \text{in } \mathcal{B} \tag{7-1}$$

and

$$\boldsymbol{L}^{\mathrm{pd}} - \boldsymbol{L}^{\mathrm{ps}} = O(\delta)O(\|\nabla\nabla \underline{T}_1\|) \quad \text{in } \mathcal{B}. \tag{7-2}$$

Proof of (7-1). Let $\boldsymbol{x} \in \mathcal{B}$ be fixed. Combining (1-8), (2-1), and (4-1) leads to

$$
\begin{aligned}
v^{\mathrm{pd}}(\boldsymbol{x}) &= \int_{\mathcal{S}} \int_0^\infty \int_0^\infty (v+w)^2 \underline{T}[\boldsymbol{x} - w\boldsymbol{m}]\langle(v+w)\boldsymbol{m}\rangle \otimes \boldsymbol{m}\, dw\, dv\, d\Omega_{\boldsymbol{m}} \\
&= \int_{\mathcal{S}} \int_0^\infty \int_0^\infty (v_1+w_1)^2 \underline{T}_1[\boldsymbol{x} - \delta w_1\boldsymbol{m}]\langle(v_1+w_1)\boldsymbol{m}\rangle \otimes \boldsymbol{m}\, dw_1\, dv_1\, d\Omega_{\boldsymbol{m}},
\end{aligned}
$$

where $v = \delta v_1$ and $w = \delta w_1$. A Taylor expansion for $\underline{T}_1$ yields

$$\underline{T}_1[\boldsymbol{x} - \delta w_1\boldsymbol{m}] = \underline{T}_1[\boldsymbol{x}] - \delta w_1 \nabla \underline{T}_1[\boldsymbol{x}]\boldsymbol{m} + \cdots.$$

After repeating the manipulations leading up to (2-4), and after evaluating the triple integral, the first term in this Taylor expansion gives the partial stress defined by (6-1). Thus

$$v^{\mathrm{pd}} = v^{\mathrm{ps}} + O(\delta)O(\|\nabla \underline{T}_1\|),$$

proving (7-1).

Proof of (7-2). Let $x \in \mathcal{B}$ be fixed. Applying a Taylor expansion to $\underline{T}[q]$ around x and setting $\xi = q - x$ leads to

$$\underline{T}[q] = \underline{T}[x] + \nabla\underline{T}[x]\xi + \tfrac{1}{2}\nabla\nabla\underline{T}[x](\xi \otimes \xi) + \cdots .$$

Combining this with (1-6), we find

$$L^{\mathrm{pd}}(x) = \int_{\mathcal{H}_x} \{\underline{T}[x]\langle\xi\rangle - \underline{T}[q]\langle-\xi\rangle\} \, dV_\xi$$

$$= \int_{\mathcal{H}_x} \left\{\underline{T}[x]\langle\xi\rangle - \left(\underline{T}[x]\langle-\xi\rangle + \nabla\underline{T}[x]\langle-\xi\rangle\xi + \tfrac{1}{2}\nabla\nabla\underline{T}[x]\langle-\xi\rangle(\xi \otimes \xi) + \cdots\right)\right\} dV_\xi.$$

Replacing ξ by $-\xi$, the first two terms in the integrand cancel. Bringing the gradient operator in the third term of the integrand outside the integral yields

$$L^{\mathrm{pd}}(x) = \nabla \cdot \int_{\mathcal{H}_x} \underline{T}[x]\langle\xi\rangle \otimes \xi \, dV_\xi - \frac{1}{2}\int_{\mathcal{H}_x} \nabla\nabla\underline{T}[x]\langle\xi\rangle(\xi \otimes \xi) \, dV_\xi + \cdots$$

$$= L^{\mathrm{ps}}(x) - \frac{1}{2}\int_{\mathcal{H}_x} \nabla\nabla\underline{T}[x]\langle\xi\rangle(\xi \otimes \xi) \, dV_\xi + \cdots .$$

Using (3-3) to express the remainder in terms of the reference force state, and setting $\xi = \delta m$, this implies

$$L^{\mathrm{pd}}(x) = L^{\mathrm{ps}}(x) - \frac{\delta}{2}\int_{\mathcal{H}_1} \nabla\nabla\underline{T}_1[x]\langle m\rangle(m \otimes m) \, dV_m + \cdots .$$

Since $|m| \leq 1$, this proves (7-2). $\qquad\square$

Because of (7-2), it follows that at the interface between subregions where L^{ps} and L^{pd} are used in the momentum balance, there are no ghost forces if the deformation is uniform (since $\underline{T}_1$ is constant in $\mathcal{B}$).

In Figure 2, we present an example of the propagation of a stress pulse in a VSH bar. The horizon increases from 0.1 on the left to 1.0 on the right through a transition region of thickness 0.1. The
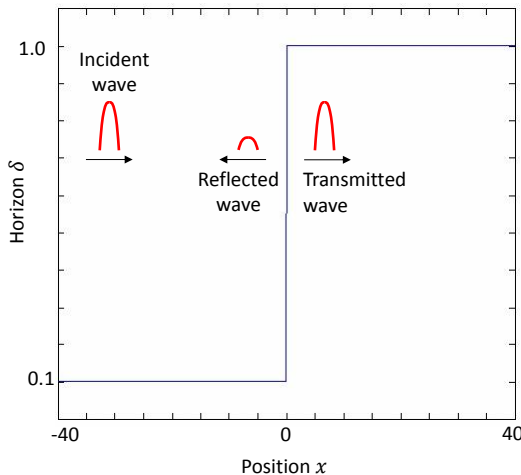
**Figure 2.** Stress pulse in a VSH bar: horizon as a function of position.
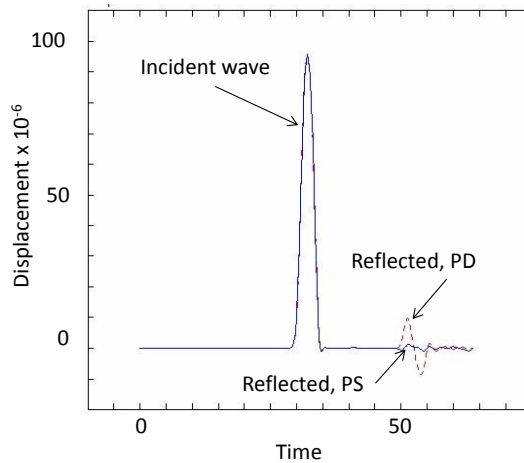
Figure 3. Stress pulse in a VSH bar: time history of displacement at $x = -10$. The two curves are for a fully peridynamic (PD) model, and for peridynamic with a partial stress (PS) region surrounding the transition in δ. The PS curve has a different reflection than the PD model.

numerical approximation method is discussed in the Appendix. An incident wave pulse is applied on the left boundary. The total thickness of the pulse is 4.0, which is thin enough that we expect to see some effect of nonlocality as the pulse moves into the high-δ region. Two cases are considered: (1) the full peridynamic equation applied throughout the domain, and (2) the partial stress model applied in a region containing and surrounding the transition region with the full peridynamic equation applied everywhere else. In case (2), the total width of the partial stress region is 10. Figure 3 compares the time history of the displacement at the point $x = -10$ for the two cases, showing both the incident and reflected pulses. Evidently, the use of the partial stress model in the transition region reduces the reflections. Figure 4 shows the comparison at the point $x = 10$, showing the transmitted pulses, which are essentially the same for both models. The change in shape of the transmitted pulse compared with the incident pulse is primarily due to nonlocality: as δ increases, short wavelength components of the pulse experience a lower wave speed. This effect of nonlocality on wave speed is reflected in the dependence on the horizon of dispersion curves for linear waves [Silling and Lehoucq 2010; Seleson and Parks 2011].

This example illustrates that it is hopeless to try to find a coupling method that transmits waves without reflection between regions with different horizons. However, as the example demonstrates, different coupling methods can have different transmission and reflection properties that may be more or less desirable for different applications.

8. Partial stress as an approximation to the local theory

In Section 7, the relationship between the partial stress and the full peridynamic versions of the internal force density were discussed. Here, we investigate the approximate relationship between the partial stress formulation and the local theory. The appropriate material model in the local theory uses the collapsed
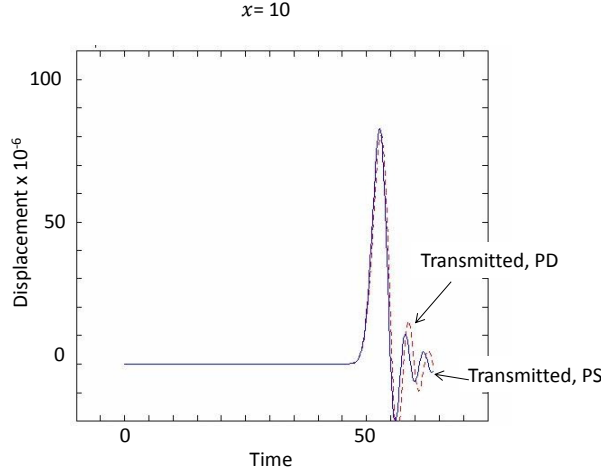
Figure 4. Stress pulse in a VSH bar: time history of displacement at $x = 10$. The transmitted pulses are similar between the two models, with the primary effect being the nonlocality of the material model.

stress tensor defined by (2-5), because, as shown in (6-5), it coincides with the partial stress for uniform deformations.

Proposition 2. *Let $\mathcal{B}$ be a homogeneous body* (*which implies constant δ*). *Let the reference material model $\widehat{\underline{T}}_1$ be a continuously differentiable function* (*of the reference deformation state*). *Let y be twice continuously differentiable in $\mathcal{B}$. Then*

$$v^{\mathrm{ps}} - v^0 = O(\delta)O(\|\nabla \underline{T}_1\|) \quad \text{in } \mathcal{B}, \tag{8-1}$$

where v^{ps} and v^0 are defined by (6-1) and (2-5), and

$$L^{\mathrm{ps}} - L^0 = O(\delta)O(\|\nabla\nabla \underline{T}_1\|) \quad \text{in } \mathcal{B}, \tag{8-2}$$

where L^{ps} and L^0 are defined by (6-2) and (2-6).

Proof of (8-1). Let $x \in \mathcal{B}$ be fixed. From (3-2) and a Taylor expansion of y around x,

$$
\begin{aligned}
\underline{Y}_1[x]\langle n \rangle &= \delta^{-1}(y(x + \delta n) - y(x)) \\
&= \delta^{-1}\big((y(x) + \delta F(x)n + \tfrac{1}{2}\delta^2 \nabla F(x)(n \otimes n) + \dots) - y(x)\big). \\
&= F(x)n + \tfrac{1}{2}\delta \nabla F(x)(n \otimes n) + \cdots.
\end{aligned}
$$

Hence,

$$\underline{Y}_1 = \underline{F} + O(\delta)O(\|\nabla \underline{F}\|), \tag{8-3}$$

and similarly

$$\nabla \underline{Y}_1 = \nabla \underline{F} + O(\delta)O(\|\nabla\nabla \underline{F}\|). \tag{8-4}$$

By the chain rule for Fréchet derivatives and (8-4),

$$
\begin{aligned}
\nabla \underline{\boldsymbol{T}}_1 &= \underline{\mathbb{K}} \bullet \nabla \underline{\boldsymbol{Y}}_1 \\
&= \underline{\mathbb{K}} \bullet (\nabla \underline{\boldsymbol{F}} + O(\delta) O(\|\nabla\nabla \underline{\boldsymbol{F}}\|)),
\end{aligned}
\tag{8-5}
$$

where $\underline{\mathbb{K}} = (\widehat{\underline{\boldsymbol{T}}}_1)_{\underline{\boldsymbol{Y}}_1}$, that is, the Fréchet derivative of $\widehat{\underline{\boldsymbol{T}}}_1$ (also known as the *micromodulus double state* [Silling 2010]). From (8-5), it is immediate that

$$
O(\|\nabla \underline{\boldsymbol{T}}_1\|) = O(\|\nabla \underline{\boldsymbol{F}}\|).
\tag{8-6}
$$

From (8-3), (8-6), and a Taylor expansion of $\widehat{\underline{\boldsymbol{T}}}_1$ near $\underline{\boldsymbol{Y}}_1$, it follows that

$$
\begin{aligned}
\widehat{\underline{\boldsymbol{T}}}_1(\underline{\boldsymbol{Y}}_1) &= \widehat{\underline{\boldsymbol{T}}}_1(\underline{\boldsymbol{F}}) + \underline{\mathbb{K}} \bullet (\underline{\boldsymbol{Y}}_1 - \underline{\boldsymbol{F}}) + \cdots \\
&= \widehat{\underline{\boldsymbol{T}}}_1(\underline{\boldsymbol{F}}) + O(\delta) O(\|\nabla \underline{\boldsymbol{F}}\|) \\
&= \widehat{\underline{\boldsymbol{T}}}_1(\underline{\boldsymbol{F}}) + O(\delta) O(\|\nabla \underline{\boldsymbol{T}}_1\|).
\end{aligned}
\tag{8-7}
$$

From (2-5), (6-4), and (8-7),

$$
\begin{aligned}
\nu^{\mathrm{ps}}(\boldsymbol{x}) &= \int_{\mathcal{H}_1} \widehat{\underline{\boldsymbol{T}}}_1(\underline{\boldsymbol{Y}}_1[\boldsymbol{x}])\langle \boldsymbol{n}\rangle \otimes \boldsymbol{n} \, dV_{\boldsymbol{n}} \\
&= \int_{\mathcal{H}_1} (\widehat{\underline{\boldsymbol{T}}}_1(\underline{\boldsymbol{F}}[\boldsymbol{x}])\langle \boldsymbol{n}\rangle + O(\delta) O(\|\nabla \underline{\boldsymbol{T}}_1\|)) \otimes \boldsymbol{n} \, dV_{\boldsymbol{n}} \\
&= \int_{\mathcal{H}_1} \widehat{\underline{\boldsymbol{T}}}_1(\underline{\boldsymbol{F}}[\boldsymbol{x}])\langle \boldsymbol{n}\rangle \otimes \boldsymbol{n} \, dV_{\boldsymbol{n}} + O(\delta) O(\|\nabla \underline{\boldsymbol{T}}_1\|) \\
&= \nu^0(\boldsymbol{x}) + O(\delta) O(\|\nabla \underline{\boldsymbol{T}}_1\|),
\end{aligned}
$$

which proves (8-1).

The proof of (8-2) is similar to that of (8-1), making use of the relations $\boldsymbol{L}^{\mathrm{ps}} = \nabla \cdot \nu^{\mathrm{ps}}$ and $\boldsymbol{L}^0 = \nabla \cdot \nu^0$. □

Since $\widehat{\underline{\boldsymbol{T}}}_1$ is constant in a VSH body under a uniform deformation, (8-1) and (8-2) imply (6-5), provided the conditions of Proposition 2 are satisfied.

Comparing (7-1) with (8-1), and comparing (7-2) with (8-2), it follows that under the conditions of Proposition 2 (which are stronger than those of Proposition 1),

$$
\nu^{\mathrm{pd}} - \nu^0 = O(\delta) O(\|\nabla \underline{\boldsymbol{T}}_1\|) \qquad \text{in } \mathcal{B},
\tag{8-8}
$$

$$
\boldsymbol{L}^{\mathrm{pd}} - \boldsymbol{L}^0 = O(\delta) O(\|\nabla\nabla \underline{\boldsymbol{T}}_1\|) \quad \text{in } \mathcal{B}.
\tag{8-9}
$$

This result is consistent with the conclusion in [Silling and Lehoucq 2008] that the collapsed internal force density is the "local limit of peridynamics".

9. A splice between two peridynamic subregions

Let two values of horizon be denoted by δ_+ and δ_-, and assume $\delta_- \leq \delta_+$. Let a reference material model $\widehat{\underline{\boldsymbol{T}}}_1$ be given. Suppose, for a given deformation, two force state fields are computed everywhere using

(3-3). For any $\boldsymbol{x} \in \mathcal{B}$, define

$$\underline{\boldsymbol{T}}_+[\boldsymbol{x}]\langle \boldsymbol{\xi} \rangle := \frac{1}{\delta_+^{1+D}} \widehat{\underline{\boldsymbol{T}}}_1(\underline{\boldsymbol{Y}}_1[\boldsymbol{x}])\left\langle \frac{\boldsymbol{\xi}}{\delta_+} \right\rangle \quad \text{and} \quad \underline{\boldsymbol{T}}_-[\boldsymbol{x}]\langle \boldsymbol{\xi} \rangle := \frac{1}{\delta_-^{1+D}} \widehat{\underline{\boldsymbol{T}}}_1(\underline{\boldsymbol{Y}}_1[\boldsymbol{x}])\left\langle \frac{\boldsymbol{\xi}}{\delta_-} \right\rangle.$$

Further suppose that $\mathcal{B}$ is divided into two disjoint subregions, $\mathcal{B}_+$ and $\mathcal{B}_-$, and assume that the internal force density at any $\boldsymbol{x} \in \mathcal{B}$ is given by

$$\boldsymbol{L}(\boldsymbol{x}) = \boldsymbol{L}^{\text{splice}}(\boldsymbol{x}) := \begin{cases} \int_{\mathcal{B}}\{\underline{\boldsymbol{T}}_+[\boldsymbol{x}]\langle \boldsymbol{q} - \boldsymbol{x}\rangle - \underline{\boldsymbol{T}}_+[\boldsymbol{q}]\langle \boldsymbol{x} - \boldsymbol{q}\rangle\}\,dV_{\boldsymbol{q}} & \text{if } \boldsymbol{x} \in \mathcal{B}_+, \\ \int_{\mathcal{B}}\{\underline{\boldsymbol{T}}_-[\boldsymbol{x}]\langle \boldsymbol{q} - \boldsymbol{x}\rangle - \underline{\boldsymbol{T}}_-[\boldsymbol{q}]\langle \boldsymbol{x} - \boldsymbol{q}\rangle\}\,dV_{\boldsymbol{q}} & \text{if } \boldsymbol{x} \in \mathcal{B}_-. \end{cases}$$

The resulting model of $\mathcal{B}$ is called a *splice* of the subregions $\mathcal{B}_+$ and $\mathcal{B}_-$.

Remark. A splice is not the same as a VSH body with $\delta(\boldsymbol{x})$ prescribed as a step function. The difference is that in a splice, a point $\boldsymbol{x}$ near the interface "sees" the force states on the other side of the interface corresponding to the same value of horizon as itself, $\delta(\boldsymbol{x})$. In contrast, in a VSH body, each point is assigned a unique value of horizon, and the force state at each point is uniquely computed according to that horizon.

In many applications, a splice provides a viable and convenient way to model a VSH body that has piecewise constant values of horizon. It is immediate that a splice model has zero internal force density under a homogeneous deformation, since the values of $\underline{\boldsymbol{T}}_+$ and $\underline{\boldsymbol{T}}_-$ are constant throughout $\mathcal{B}_+$ and $\mathcal{B}_-$, respectively. This implies that a splice model produces no ghost forces under a uniform deformation. This is the main advantage of a splice over a VSH body. The splice is similar to an adaptivity concept for 1D bond-based peridynamics proposed by Bobaru et al. [2009] and in 2D by Bobaru and Ha [2011]. A related approach has been used in the context of atomistic-to-continuum coupling by Seleson and Gunzburger [2010].

It follows from Proposition 2 that in a splice, recalling that $\delta_- \leq \delta_+$,

$$v_+^{\text{pd}} - v_-^{\text{pd}} = O(\delta_+)O(\|\nabla \underline{\boldsymbol{T}}_1\|) \quad \text{on } \mathcal{B}$$

and

$$\boldsymbol{L}_+^{\text{pd}} - \boldsymbol{L}_-^{\text{pd}} = O(\delta_+)O(\|\nabla\nabla \underline{\boldsymbol{T}}_1\|) \quad \text{on } \mathcal{B},$$

provided that the conditions of Proposition 2 are satisfied.

10. Local-nonlocal coupling

The situation frequently arises that we wish to model most of a body using the classical (local) theory, and only a small portion (such as in the vicinity of a growing crack) with peridynamics. A method for achieving the transition between the two is referred to as *local–nonlocal coupling*. Methods that have been proposed for local–nonlocal coupling include Arlequin [Han and Lubineau 2012], morphing [Lubineau et al. 2012; Azdoud et al. 2013; 2014], and blending [Seleson et al. 2013a; 2015]. Liu and Hong [2012] proposed a coupling method using interface elements. Methods that achieve coupling by treating peridynamic bonds as finite elements are described in [Macek and Silling 2007] and [Oterkus et al. 2012], which contains additional references. Related issues in nonlocal diffusion were investigated by Seleson, Gunzburger, and Parks [2013b]. Wu [2014] investigated a local–nonlocal coupling method

for correspondence materials in state-based peridynamics. An adaptive method for coupling peridynamic and local regions is discussed by Wildman and Gazonas [2014].

One option for local–nonlocal coupling is to use the partial stress field as a bridge between local and peridynamic subregions. In this approach, $\mathcal{B}$ is divided into three disjoint subregions $\mathcal{B}_0$, $\mathcal{B}_{\mathrm{ps}}$, and $\mathcal{B}_{\mathrm{pd}}$. To avoid ghost forces under a uniform deformation, $\delta > 0$ is assumed to be constant in $\mathcal{B}_{\mathrm{pd}}$. Changes in δ occur entirely within $\mathcal{B}_{\mathrm{ps}}$, such that δ is continuous in $\mathcal{B}$. (Recall from (6-5) that $\nu^{\mathrm{ps}} \equiv \nu^0$ and $\boldsymbol{L}^{\mathrm{ps}} \equiv \boldsymbol{L}^0$ where $\delta \equiv 0$.) The internal force density is given by

$$\boldsymbol{L}(\boldsymbol{x}) = \begin{cases} \boldsymbol{L}^{\mathrm{pd}}(\boldsymbol{x}) & \text{if } \boldsymbol{x} \in \mathcal{B}_{\mathrm{pd}}, \\ \boldsymbol{L}^{\mathrm{ps}}(\boldsymbol{x}) & \text{if } \boldsymbol{x} \in \mathcal{B}_{\mathrm{ps}}, \\ \boldsymbol{L}^0(\boldsymbol{x}) & \text{if } \boldsymbol{x} \in \mathcal{B}_0. \end{cases} \qquad (10\text{-}1)$$

The convergence properties of this method are given by (7-2) and (8-2).

Another option for local–nonlocal coupling is to use the idea of a splice described in Section 9. The body is divided into two disjoint subregions $\mathcal{B}_0$ and $\mathcal{B}_{\mathrm{pd}}$ that use the local model and the full peridynamic model (constant $\delta > 0$), respectively. The internal force density in the splice model is given by

$$\boldsymbol{L}(\boldsymbol{x}) = \begin{cases} \boldsymbol{L}^{\mathrm{pd}}(\boldsymbol{x}) & \text{if } \boldsymbol{x} \in \mathcal{B}_{\mathrm{pd}}, \\ \boldsymbol{L}^0(\boldsymbol{x}) & \text{if } \boldsymbol{x} \in \mathcal{B}_0. \end{cases} \qquad (10\text{-}2)$$

The convergence properties of such a splice model are given by (8-9).

These two options for local–nonlocal coupling differ primarily in the way they transmit waves whose wavelength is smaller than or on the order of δ. As illustrated in the example in Section 7, the transition from a local region to a nonlocal region involves a change in the dispersion properties of the material, resulting in reflections of waves. However, because the partial stress coupling method (10-1) allows a gradual change in length scale, it can be used to reduce wave reflections compared to the splice approach (10-2). As discussed in the Appendix, numerical computation of $\boldsymbol{L}^{\mathrm{ps}}$ requires the suppression of zero energy mode oscillations, similar to correspondence material models [Littlewood 2010; 2011; Breitenfeld et al. 2014]. The root cause of these oscillations is the noninvertibility of $\hat{\nu^{\mathrm{ps}}}(\underline{\boldsymbol{Y}})$, that is, there are many possible deformations of the family that result in the same partial stress tensor.

As an example, we apply these two methods for local–nonlocal coupling to the problem of spall initiated by the impact of two brittle elastic plates. The impactor has half the thickness of the target and strikes the target from the left side. As shown in the wave diagram in Figure 5, the compressive waves that issue from the contact surface between the impactor and the target eventually intersect each other at the midplane of the target plate. When this happens, the waves, which by that time are both tensile, reinforce each other to create a thin region where the stress is strongly tensile. Within this tensile region, the strength of the material is exceeded and a crack forms. The formation of this crack creates release pulses that move in both directions. The velocity induced by the rightward-moving release pulse as it reflects from the free surface of the target bar can be measured using VISAR or other techniques [Field et al. 2004]. With the help of analysis or computational modeling, the exact characteristics of the crack release (or "pullback") pulse can be interpreted using suitable data processing techniques to reveal the dynamic strength properties of materials under strong tension (spall).

In the computational model of this spall experiment, the impactor and target plates have thicknesses of 20 and 40, respectively. The numerical solution method is described in the Appendix. The impact
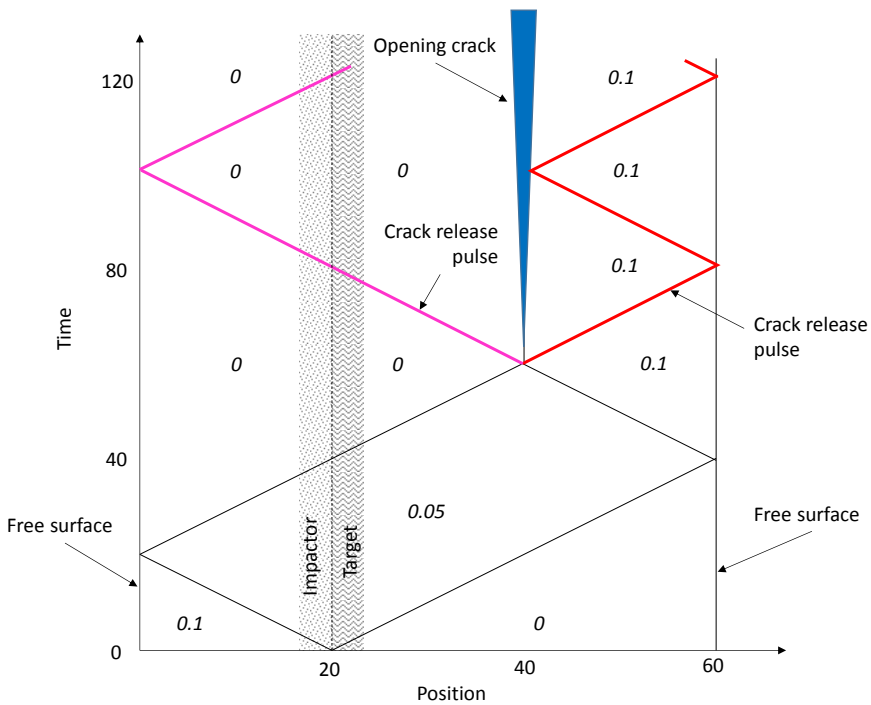
Figure 5. Wave diagram for the impact of a plate (from the left) on a target plate. Waves reinforce at the midplane of the target plate to cause fracture. Numbers in italics represent particle velocity.

velocity is 0.1. The elastic modulus and density of both plates are 1. The reference material model $\widehat{\underline{T}}_1$ is chosen to be the bond-based prototype microelastic brittle (PMB) material model [Silling and Askari 2005] with a critical bond strain for failure of 0.04. The entire region is discretized into 1000 nodes. The objective is to model the relatively small part of the body where damage can occur using the full peridynamic equations. This peridynamic region is coupled to local regions using either of the following two methods:

- Partial stress: a peridynamic region of thickness 10, centered at the midpoint of the target plate, is enclosed by layers of thickness 4 where the partial stress method is applied. Beyond this, the local equations are used. In the peridynamic and partial stress regions, the horizon is $\delta = 0.13$.

- Splice: a peridynamic region of thickness 10 and horizon $\delta = 0.13$, centered at the midpoint of the target plate, is spliced to local regions.

For comparison, results using the full peridynamic model in the entire domain ($\delta = 0.13$ throughout) are also computed.

The computed velocity profile at time $t = 70$, using the splice method for local–nonlocal coupling, is shown in Figure 6. Comparing this figure with the wave diagram in Figure 5, a number of salient features may be seen. The crack appears as a sharp jump in velocity as a function of position at $x = 40$.
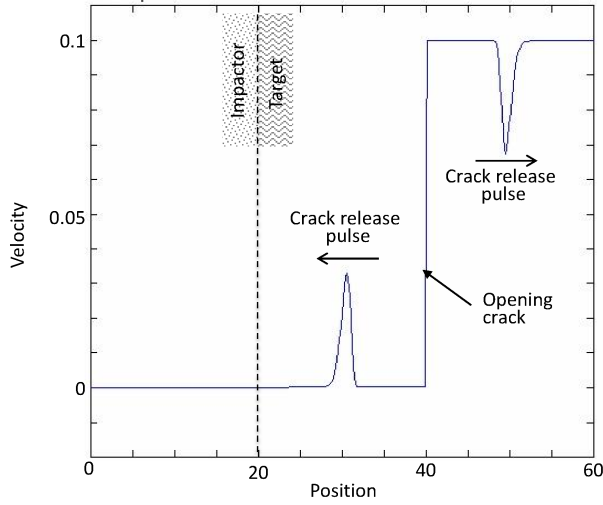
Figure 6. Velocity as a function of position at $t = 70$ in the spall example problem using the splice method for local–nonlocal coupling. There are no significant artifacts from the local–nonlocal transitions, which are located at $x = 37$ and $x = 43$.
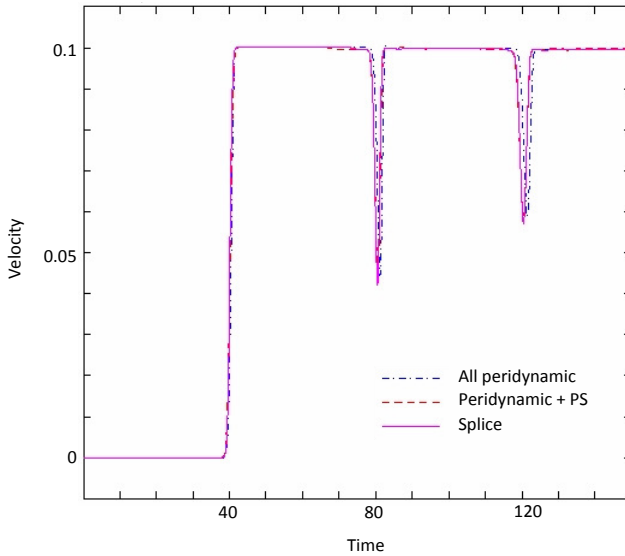
Figure 7. Velocity history at the free (right) surface of the target plate, showing the release pulse from the dynamic fracture occurring in the interior of the target bar. The three curves are for fully peridynamic (PD), local–nonlocal coupling using partial stress (PS), and local–nonlocal coupling using a splice.

The two release (pullback) pulses move away from the crack at the wave velocity, which is $c = 1.0$. In Figure 5, the particle velocities are indicated with italic numbers. The computed velocity history at the free surface is shown in Figure 7 for the two local–nonlocal coupling methods, partial stress (PS) and

splice, along with the full peridynamic model. The dips in velocity represent the crack release pulse created in the interior of the target due to spall.

As demonstrated in Figure 7, the three methods give nearly the same results in this example. However, a fully peridynamic model in multiple dimensions would require a much higher computational cost than either of the proposed local–nonlocal coupling methods, due to the large number of nonlocal interactions required to discretize the material model. So, in multiple dimensions, in problems where damage is confined to a small subregion, the splice or partial stress methods potentially offer a significant reduction in computational cost, while avoiding ghost forces. This anticipated cost reduction is a primary motivation for development of local–nonlocal coupling methods.

11. Discussion

In this paper, we proposed a notion of a homogeneous body (a "variable scale homogeneous" body) that characterizes a peridynamic medium with variable horizon but constant bulk material properties. We analyzed the origin and effect of ghost forces due to changes in the horizon in the full peridynamic model. The importance of these ghost forces depends on the application; they may or may not be acceptable in a computational simulation. These anomalies can be reduced by making $\delta(\boldsymbol{x})$ a smoothly varying function.

If the ghost forces under a uniform deformation are not acceptable, the partial stress field can be used to effect a transition between regions with different horizons. The partial stress field appears in a modified form of the equilibrium equation. The partial stress approaches the collapsed stress in the limit of zero horizon, if the deformation is continuously differentiable. The collapsed stress, $\hat{\nu}^0(\boldsymbol{F})$, provides a material model for the first Piola–Kirchhoff stress in the local formulation.

The partial stress formulation is not thermodynamically consistent in the sense that along a cyclic loading path of a family in an elastic material, nonzero net work may appear:

$$\oint \nu^{\widehat{\mathrm{ps}}}(\underline{\boldsymbol{Y}}) \cdot d\boldsymbol{F} \neq 0. \tag{11-1}$$

(An exception to this is a uniform deformation, in which case $\underline{\boldsymbol{Y}} = \underline{\boldsymbol{F}}$.) The root cause of this inconsistency, which is evident in (11-1), is that the partial stress concept mixes local and nonlocal kinematics. The partial stress is therefore not suitable as a basis for a general theory of continuum mechanics. The full peridynamic theory, like the local theory, *is* thermodynamically consistent [Silling and Lehoucq 2010; Oterkus et al. 2014a; 2014b], that is,

$$\oint \widehat{\underline{\boldsymbol{T}}}(\underline{\boldsymbol{Y}}) \bullet d\underline{\boldsymbol{Y}} = 0 \quad \text{and} \quad \oint \hat{\nu}^0(\boldsymbol{F}) \cdot d\boldsymbol{F} = 0.$$

To connect subregions with constant δ to each other, or to achieve local–nonlocal coupling, subregions can be connected using a splice. This method allows the peridynamic material model in each subregion to "see" force states in the other subregion with the same horizon as itself. The methods proposed in this paper may provide a means to reduce the computational cost of modeling a crack with peridynamics by connecting it to a larger surrounding region that is modeled with the local theory.

Appendix: Computational details

All the numerical examples in this paper involving nonlocal models used the method described in [Silling and Askari 2005]. This method uses a midpoint quadrature rule in a Lagrangian discretization of the body. The approximation in one dimension for the peridynamic internal force density is

$$L_i^{\text{pd}} = \sum_{j \in \mathcal{F}_i} (T_{ij} - T_{ji}) V_j,$$

where i and j are node numbers, V_j is the volume of node j, $\mathcal{F}_i$ is the set of nodes in the material family of i, and

$$T_{ij} = \widehat{\underline{T}}(\underline{Y}[x_i], x_i)\langle x_j - x_i \rangle, \qquad T_{ji} = \widehat{\underline{T}}(\underline{Y}[x_j], x_j)\langle x_i - x_j \rangle,$$

$$\underline{Y}[x_i]\langle x_j - x_i \rangle = y_j - y_i, \qquad \underline{Y}[x_j]\langle x_i - x_j \rangle = y_i - y_j.$$

The partial stress is computed as

$$v_i^{\text{ps}} = \sum_{j \in \mathcal{F}_i} T_{ij}(x_j - x_i) V_j.$$

The partial stress internal force density is approximated by

$$L_i^{\text{ps}} = \frac{v_{i+1}^{\text{ps}} - v_{i-1}^{\text{ps}}}{2\Delta x},$$

where Δx is the mesh spacing. For computations involving the PDEs of the local theory, the Piola (collapsed) stress is approximated by the finite difference formula

$$v_{i+1/2}^0 = \hat{v}^0(F_{i+1/2}) \quad \text{with} \quad F_{i+1/2} = \frac{y_{i+1} - y_i}{\Delta x}.$$

where $\hat{v}^0$ is the material model for the Piola stress. The internal force density in the local model is approximated by

$$L_i^0 = \frac{v_{i+1/2}^0 - v_{i-1/2}^0}{\Delta x}.$$

For dynamics, time integration is performed using explicit central differencing:

$$v_i^{n+1/2} - v_i^{n-1/2} = a_i^n \Delta t,$$

$$y_i^{n+1} - y_i^n = v_i^{n+1/2} \Delta t,$$

where Δt is the time step size. At time step n, the acceleration is computed from

$$\rho a_i^n = L_i^n + b_i^n + \eta_i^n,$$

where L is either L^{pd}, L^{ps}, or L^0, ρ is mass density, b is a prescribed body force density, and η is a linear artificial viscosity:

$$\eta_i^n = \alpha \rho c \Delta x (v_{i+1}^n - 2v_i^n + v_{i-1}^n),$$

where c is the wave speed and α is a dimensionless constant on the order of $1/4$. The linear artificial viscosity is effective in reducing zero energy mode oscillations that can appear due to the noninvertibility of the partial stress tensor and, when a correspondence material model is used, of the peridynamic force state. Other methods for controlling zero energy mode oscillations are described by Breitenfeld et al. [2014]

and by Littlewood [2010; 2011]. The artificial viscosity η_i^n is not applied if the bonds from i to $i + 1$ or i to $i - 1$ are damaged according to the material damage model at time step n. Otherwise, the artificial viscosity would create nonphysical forces across a crack surface.

References

[Azdoud et al. 2013] Y. Azdoud, F. Han, and G. Lubineau, "A morphing framework to couple non-local and local anisotropic continua", *Int. J. Solids Struct.* **50**:9 (2013), 1332–1341.

[Azdoud et al. 2014] Y. Azdoud, F. Han, and G. Lubineau, "The morphing method as a flexible tool for adaptive local/non-local simulation of static fracture", *Comput. Mech.* **54**:3 (2014), 711–722.

[Bobaru and Ha 2011] F. Bobaru and Y. Ha, "Adaptive refinement and multiscale modeling in 2D peridynamics", *Int. J. Multiscale Comput. Eng.* **9** (2011), 707–726.

[Bobaru et al. 2009] F. Bobaru, M. Yang, L. F. Alves, S. A. Silling, E. Askari, and J. Xu, "Convergence, adaptive refinement, and scaling in 1D peridynamics", *Int. J. Numer. Methods Eng.* **77**:6 (2009), 852–877.

[Breitenfeld et al. 2014] M. S. Breitenfeld, P. H. Geubelle, O. Weckner, and S. A. Silling, "Non-ordinary state-based peridynamic analysis of stationary crack problems", *Comput. Methods Appl. Mech. Eng.* **272** (2014), 233–250.

[Field et al. 2004] J. Field, S. Walley, W. Proud, H. Goldrein, and C. Siviour, "Review of experimental techniques for high rate deformation and shock studies", *Int. J. Impact Eng.* **30**:7 (2004), 725–775.

[Han and Lubineau 2012] F. Han and G. Lubineau, "Coupling of nonlocal and local continuum models by the Arlequin approach", *Int. J. Numer. Methods Eng.* **89**:6 (2012), 671–685.

[Lehoucq and Silling 2008] R. B. Lehoucq and S. A. Silling, "Force flux and the peridynamic stress tensor", *J. Mech. Phys. Solids* **56**:4 (2008), 1566–1577.

[Littlewood 2010] D. J. Littlewood, "Simulation of dynamic fracture using peridynamics, finite element modeling, and contact", pp. 209–217 in *ASME 2010 International Mechanical Engineering Congress and Exposition* (Vancouver, 2010), 2010.

[Littlewood 2011] D. J. Littlewood, "A nonlocal approach to modeling crack nucleation in AA 7075-T651", pp. 567–576 in *ASME 2011 International Mechanical Engineering Congress and Exposition* (Denver, CO, 2011), 2011.

[Liu and Hong 2012] W. Liu and J.-W. Hong, "A coupling approach of discretized peridynamics with finite element method", *Comput. Methods Appl. Mech. Eng.* **245/246** (2012), 163–175.

[Lubineau et al. 2012] G. Lubineau, Y. Azdoud, F. Han, C. Rey, and A. Askari, "A morphing strategy to couple non-local to local continuum mechanics", *J. Mech. Phys. Solids* **60**:6 (2012), 1088–1102.

[Macek and Silling 2007] R. W. Macek and S. A. Silling, "Peridynamics via finite element analysis", *Finite Elem. Anal. Des.* **43**:15 (2007), 1169–1178.

[Oterkus et al. 2012] E. Oterkus, E. Madenci, O. Weckner, S. Silling, P. Bogert, and A. Tessler, "Combined finite element and peridynamic analyses for predicting failure in a stiffened composite curved panel with a central slot", *Compos. Struct.* **94**:3 (2012), 839 – 850.

[Oterkus et al. 2014a] S. Oterkus, E. Madenci, and A. Agwai, "Fully coupled peridynamic thermomechanics", *J. Mech. Phys. Solids* **64** (2014), 1–23.

[Oterkus et al. 2014b] S. Oterkus, E. Madenci, and A. Agwai, "Peridynamic thermal diffusion", *J. Comput. Phys.* **265** (2014), 71–96.

[Seleson and Gunzburger 2010] P. Seleson and M. Gunzburger, "Bridging methods for atomistic-to-continuum coupling and their implementation", *Commun. Comput. Phys.* **7**:4 (2010), 831–876.

[Seleson and Parks 2011] P. Seleson and M. Parks, "On the role of the influence function in the peridynamic theory", *Int. J. Multiscale Comput. Eng.* **9** (2011), 689–706.

[Seleson et al. 2013a] P. Seleson, S. Beneddine, and S. Prudhomme, "A force-based coupling scheme for peridynamics and classical elasticity", *Comput. Mater. Sci.* **66** (2013), 34–49.

[Seleson et al. 2013b] P. Seleson, M. Gunzburger, and M. L. Parks, "Interface problems in nonlocal diffusion and sharp transitions between local and nonlocal domains", *Comput. Methods Appl. Mech. Eng.* **266** (2013), 185–204.

[Seleson et al. 2015] P. Seleson, Y. D. Ha, and S. Beneddine, "Concurrent coupling of bond-based peridynamics and the Navier equation of classical elasticity by blending", *J. Multiscale Comput. Eng.* **13** (2015), 91–113.

[Silling 2000] S. A. Silling, "Reformulation of elasticity theory for discontinuities and long-range forces", *J. Mech. Phys. Solids* **48**:1 (2000), 175–209.

[Silling 2010] S. A. Silling, "Linearized theory of peridynamic states", *J. Elasticity* **99**:1 (2010), 85–111.

[Silling and Askari 2005] S. Silling and E. Askari, "A meshfree method based on the peridynamic model of solid mechanics", *Comput. Struct.* **83**:17-18 (2005), 1526–1535.

[Silling and Lehoucq 2008] S. A. Silling and R. B. Lehoucq, "Convergence of peridynamics to classical elasticity theory", *J. Elasticity* **93**:1 (2008), 13–37.

[Silling and Lehoucq 2010] S. Silling and R. Lehoucq, "Peridynamic theory of solid mechanics", pp. 73 – 168 in *Advances in Applied Mechanics*, vol. 44, edited by H. Aref and E. van der Giessen, Elsevier, 2010.

[Silling et al. 2007] S. A. Silling, M. Epton, O. Weckner, J. Xu, and E. Askari, "Peridynamic states and constitutive modeling", *J. Elasticity* **88**:2 (2007), 151–184.

[Wildman and Gazonas 2014] R. Wildman and G. Gazonas, "A finite difference-augmented peridynamics method for reducing wave dispersion", *Int. J. Fract.* **190**:1-2 (2014), 39–52.

[Wu 2014] C. T. Wu, "Kinematic constraints in the state-based peridynamics with mixed local/nonlocal gradient approximations", *Comput. Mech.* **54**:5 (2014), 1255–1267.

STEWART A. SILLING: sasilli@sandia.gov
Multiscale Science Department, Sandia National Laboratories, P.O. Box 5800, MS 1322, Albuquerque, NM 87185-1320, United States

DAVID J. LITTLEWOOD: djlittl@sandia.gov
Multiscale Science Department, Sandia National Laboratories, P.O. Box 5800, MS 1322, Albuquerque, NM 87185-1320, United States

PABLO SELESON: selesonpd@ornl.gov
Computer Science and Mathematics Division, Oak Ridge National Laboratory, P.O. Box 2008, Oak Ridge, TN 37831, United States

JOURNAL OF MECHANICS OF MATERIALS AND STRUCTURES

Founded by Charles R. Steele and Marie-Louise Steele

Cover photo: Wikimedia Commons

Special issue on
Peridynamic Theory